

# 转子—电磁轴承非线性系统时滞减振研究<sup>\*</sup>

张国荣 王希奎 邹瀚森 张勇 席光<sup>†</sup>

(西安交通大学 能源与动力工程学院, 西安 710049)

**摘要** 电磁轴承具有与转子无接触、可施加主动控制等特性,越来越多地被应用于高速旋转机械的支撑与减振。为了研究转子—电磁轴承系统中时滞的减振作用,在主共振情况下推导了八极电磁轴承支撑的转子非线性振动方程。应用多尺度法获得了振动方程的近似解,并利用 Lyapunov 方法对解的稳定性进行判定。结果表明,时滞的某些取值会使转子在  $x$  和  $y$  方向上的振幅相对于无时滞时减小,称之为时滞的“减振区域”,并且  $x$  和  $y$  方向上“减振区域”不同;通过计算不同比例系数与微分系数下的时滞—振幅曲线,发现比例系数对“减振区域”的范围影响更大;同一时滞量参数不能保证所有转速下均减振,当时滞量选取不合适时,会造成系统失稳;通过计算偏心率—振幅曲线,发现时滞控制能有效降低由于转子不平衡所产生的振幅,并且消除了非线性现象如多值、突跳等,系统稳定性增加。数值模拟验证了解析结果的正确性。

**关键词** 电磁轴承, 时滞, 振动控制, 多尺度法

中图分类号:TH133.3

文献标志码:A

## Vibration Suppression of Time Delay in Rotor-Magnetic Bearing Nonlinear System<sup>\*</sup>

Zhang Guorong Wang Xikui Zou Hansen Zhang Yong Xi Guang<sup>†</sup>

(School of Mathematics and Statistics, North China University of Water Resources and Electric Power, Zhengzhou 450045, China)

**Abstract** Active magnetic bearing (AMB) has the characteristics of no contact with the rotor and can be applied to active control. It is more and more used in the support and vibration reduction of high-speed rotating machinery. In order to study the vibration suppression of the time delay in the rotor-magnetic bearing system, the nonlinear vibration equation of the rotor supported by the eight-pole legs magnetic bearing is derived based on the primary resonance. The method of multiple scales is applied to obtain the approximate solution of the vibration equation and the stability of the solution is also analyzed by Lyapunov principle. The ‘vibration suppression area’ of the time delay is defined as the range in which the stable vibration amplitude is less than the amplitude when the time delay is zero. The study found that proportional gain has a greater impact on the ‘vibration suppression area’ of the time delay relative to derivative gain by the time delay-amplitude curves at different proportional gains and derivative gains. The same time delay cannot guarantee suppressing vibration at all speeds, and if the time delay is not selected properly, it will cause system instability. By calculating the eccentricity-amplitude curves, it is found that the time delay control can effectively reduce the amplitude due to rotor unbalance and eliminate the nonlinear phenomena such as multiple values and jumping, and the system stability increases. Numerical simulations verify the correctness of the analytical results.

**Key words** active magnetic bearing, time delay, vibration suppression, the method of multiple scales

## 引言

旋转机械是工业生产中最重要设备之一,在大部分工业系统中都发挥基础性的作用,其工作性能的好坏直接关系到整个系统的效率高低.主动电磁轴承因其优良的特性如:转子与定子不接触、可施加主动控制等越来越多地被应用于旋转轴的支撑中.但电磁轴承具有开环不稳定性,需要对其进行闭环控制,并且控制方法很大程度上决定了电磁轴承的工作性能.很多先进的控制方法已被应用到电磁轴承系统中,如滑模控制、 $H_\infty$ 鲁棒控制、模糊控制、神经网络等.上述方法相对于传统的PID控制来说具有更好的控制性能及减振效果,但也存在控制器阶数较高、物理意义不明显等短板,因此还未在实际电磁轴承系统中广泛应用.

近年来,时滞控制越来越多的被用于减振.时滞存在于各类控制系统中,在信号的采集、输送以及处理过程中不可避免地会产生一定的时滞<sup>[1]</sup>.系统中时滞的存在可能会使系统性能变差<sup>[2]</sup>, Ji等<sup>[3]</sup>理论分析了转子—电磁轴承系统的主共振情况,并分析了时滞对稳定性的影响,发现随着时滞量的增加,系统振动幅值增大,稳定解会通过Hopf分岔失稳.近年来,研究人员发现当时滞量取某些值时能对系统的振动起抑制作用.时滞控制就是在控制器中添加主动时滞以达到系统减振的效果.Saeed等<sup>[4-6]</sup>利用时滞饱和控制器去控制梁和转子的振动,发现当时滞量取某些值时,系统的振动被抑制.刘显波<sup>[7]</sup>利用时滞状态反馈改进了PID控制器去控制纵扭耦合的钻柱系统,发现改进后的控制器使系统稳定域扩大.Amer等<sup>[8-9]</sup>利用时滞反馈控制器成功减小了Duffing振子和Rayleigh-vander Pol-Duffing振子的振动幅值.赵艳影等<sup>[10]</sup>研究了时滞非线性动力吸振器的减振作用,发现当参数都调整合适时,系统振动较无时滞可减小90%左右.为推进时滞反馈控制的实际应用,Yan等<sup>[11]</sup>设计了实验平台去研究车辆支撑系统中考虑时滞的最优控制规律,研究结果表明合适的时滞量会降低系统幅值,但时滞量与振动幅值之间为高度非线性

关系.邵素娟等<sup>[12]</sup>利用时滞减振技术成功减小了车辆主动悬架系统的振动,其运用多尺度法建立了系统的非线性模型,并研究了系统参数对系统稳定性的影响.

以上展示了近年来研究人员对于时滞控制的研究进展,但在高速转子—电磁轴承系统中时滞对系统的影响以及减振研究报道还较少,因此,本文主要研究时滞反馈控制在转子—电磁轴承系统中的应用.首先建立了时滞状态反馈的转子振动方程;其次利用多尺度法推导出转子在主共振情况下振动方程的近似解并进行稳定性判定;然后详细分析了不同时滞量对振动幅值和稳定性的影响,研究了控制参数对时滞“减振区域”的影响,以及在不同转速、不同质量偏心率下时滞减振的效果;最后通过数值计算验证了近似解的准确性.

## 1 建立模型

图1为转子—电磁轴承闭环系统示意图.电涡流传感器获得转子位移;控制器根据转子位移计算出相应控制电压;功率放大器根据控制电压的大小产生相应的控制电流 $I_c$ .系统采用差动驱动模式,即一个磁铁由偏置电流 $I_0$ 与控制电流 $I_c$ 的和驱动,另一个磁铁由两者之差驱动,由此产生电磁力对转子进行主动控制.

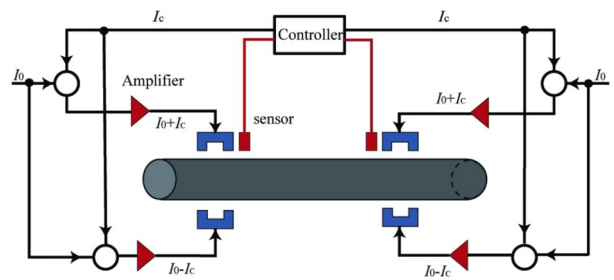


图1 转子—电磁轴承系统示意图

Fig.1 Schematic diagram of rotor-active magnetic bearing system

### 1.1 方程推导

图2为转子—八极电磁轴承系统的截面图.转子为刚性转子模型,忽略磁泄露、涡流效应等对本文研究目标影响较小的因素.

第 $j$  ( $j=1, 2, 3, 4$ )个磁极对的电磁力<sup>[13]</sup>为

$$F_j(I_j, \omega_j) = -\frac{\mu_0 A_a N^2}{4} \left[ \frac{(I_0 + I_j)^2}{(C_0 + \omega_j)^2} - \frac{(I_0 - I_j)^2}{(C_0 - \omega_j)^2} \right] \cos\theta, \quad j = 1, 2, 3, 4 \quad (1)$$

其中,  $\mu_0$  为真空磁导率,  $A_a$  是磁极的横截面积,  $N$  是线圈匝数,  $I_0$  代表偏置电流,  $I_j$  是第  $j$  个磁极对的控制电流,  $C_0$  是磁极与转子的额定间隙,  $\omega_j$  是第  $j$  个方向的转子位移,  $\theta$  代表电磁力作用在转子上的角度。

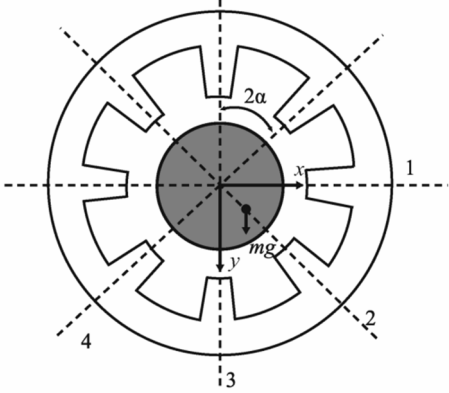


图 2 转子-八极电磁轴承系统截面图

Fig.2 Sectional view of rotor-eight pole legs magnetic bearing system

采用时滞状态反馈的 PD 控制,有

$$I_c = k_p \omega(t - \tau_1) + k_d \dot{\omega}(t - \tau_2) \quad (2)$$

其中,  $\tau_1$  为位移信号总时滞,  $\tau_2$  为速度信号总时滞,  $k_p$  为位移增益,  $k_d$  为速度增益。

图 2 中磁极与磁极之间夹角  $2\alpha = \pi/4$ , 因此转子在第  $j$  个磁极对方向的位移与相应控制电流为

$$\begin{aligned} \omega_1 &= x, I_1 = i_1, \\ \omega_2 &= x \cos\left(\frac{\pi}{4}\right) + y \sin\left(\frac{\pi}{4}\right), I_2 = i_0 + i_2 \\ \omega_3 &= y, I_3 = i_0 + i_3, \\ \omega_4 &= x \cos\left(\frac{3\pi}{4}\right) + y \sin\left(\frac{3\pi}{4}\right), I_4 = i_0 + i_4 \end{aligned} \quad (3)$$

$x, y$  方向电磁力合力为

$$\begin{aligned} F_x &= F_1 + F_2 \cos \frac{\pi}{4} + F_4 \cos \frac{3\pi}{4} \\ F_y &= F_3 + F_2 \sin \frac{\pi}{4} + F_4 \sin \frac{3\pi}{4} \end{aligned} \quad (4)$$

其中,  $F_j (j=1, 2, 3, 4)$  代表图 2 中  $j$  方向磁极对的电磁力. 将(1)~(3)带入(4)可得到电磁力的具体形式。

转子在  $x$  和  $y$  方向上振动方程为

$$\begin{aligned} m\ddot{x} &= F_x - c\dot{x} + m\epsilon\Omega^2 \cos(\Omega t) \\ m\ddot{y} &= F_y - c\dot{y} + m\epsilon\Omega^2 \sin(\Omega t) + mg \end{aligned} \quad (5)$$

其中  $m, c, e, \Omega, g$  分别为转子质量、转子阻尼系数、质量偏心率、转速、重力加速度,  $F_x$  为水平方向电磁力合力,  $F_y$  为竖直方向电磁力合力。

引入下列无量纲量

$$\begin{aligned} x^* &= \frac{x}{C_0}, y^* = \frac{y}{C_0}, t^* = \sqrt{\frac{a}{mC_0}} t, \\ \tau_1^* &= \sqrt{\frac{a}{mC_0}} \tau_1, \tau_2^* = \sqrt{\frac{a}{mC_0}} \tau_2, \\ \Omega^* &= \sqrt{\frac{mC_0}{a}} \Omega, k_p^* = \frac{k_p C_0}{I_0}, \\ k_d^* &= \frac{k_d C_0}{I_0} \sqrt{\frac{a}{mC_0}}, c^* = \frac{cC_0}{a} \sqrt{\frac{a}{mC_0}}, \\ e^* &= \frac{e}{C_0}, i_0^* = \frac{i_0}{I_0} \end{aligned} \quad (6)$$

其中  $a = \frac{\mu_0 A_a N^2 I_0^2}{4C_0^2} \cos\theta$ 。

当转子稳定在中心即  $y = 0$  时,  $y$  方向电磁力合力应与重力平衡<sup>[13]</sup>, 故有

$$\begin{aligned} mg &= \frac{(\sqrt{2} + 1)\mu_0 AN^2}{4} \left[ \frac{(I_0 + i_0)^2}{C_0^2} - \frac{(I_0 - i_0)^2}{C_0^2} \right] \cos\theta \\ &= 4(\sqrt{2} + 1)ai_0^* \end{aligned} \quad (7)$$

将式(4), 式(6), 式(7)带入式(5), 得到无量纲振动方程, 见附录公式(1). 为方便表述, 略去“\*”, 以下公式推导中符号均为无量纲形式. 将得到的无量纲振动方程进行 Taylor 展开到三阶. 由于有时滞项的存在, 难以直接表示  $x$  和  $y$  方向上固有频率, 因此进行以下处理<sup>[14]</sup>

$$\begin{aligned} 8k_p x_{\tau_1} &= 8k_p \left[ x - \int_{t-\tau_1}^t \dot{x}(\sigma) d\sigma \right] \approx 8k_p (x - \tau_1 \dot{x}) \\ 8k_p y_{\tau_1} &= 8k_p \left[ y - \int_{t-\tau_1}^t \dot{y}(\sigma) d\sigma \right] \approx 8k_p (y - \tau_1 \dot{y}) \end{aligned} \quad (8)$$

为应用多尺度法, 在上述 Taylor 展开后的无量纲方程中引入小参数  $\epsilon$  整理得

$$\begin{aligned} \ddot{x} + \omega_x^2 x + \epsilon \mu \dot{x} - \epsilon (\mu_1 \dot{y}_{\tau_2} + \alpha_1 y_{\tau_1} + 3\mu_2 \dot{x}_{\tau_2}^2 + \mu_2 \dot{y}_{\tau_2}^2 + 3\mu_3 x_{\tau_1} \dot{x}_{\tau_2} + \mu_3 y_{\tau_1} \dot{y}_{\tau_2} + 3\alpha_2 x_{\tau_1}^2 + \alpha_2 y_{\tau_1}^2) x - \epsilon (\mu_1 \dot{x}_{\tau_2} + 2\mu_2 \dot{x}_{\tau_2} \dot{y}_{\tau_2} + \mu_3 \dot{x}_{\tau_2} y_{\tau_1} + \alpha_1 x_{\tau_1} + \mu_3 x_{\tau_1} \dot{y}_{\tau_2} + 2\alpha_2 x_{\tau_1} y_{\tau_1}) y + \epsilon (9\mu_4 \dot{x}_{\tau_2} x^2 + 3\alpha_3 x_{\tau_1} x^2 + 3\mu_4 \dot{x}_{\tau_2} y^2 + \alpha_3 x_{\tau_1} y^2 + 2\beta_3 xy + 6\mu_4 x y \dot{y}_{\tau_2} + 2\alpha_3 x y y_{\tau_1} - \beta_1 x^3 - \beta_2 x y^2 + 4\mu_4 \dot{x}_{\tau_2}) = \epsilon \epsilon \Omega^2 \cos \Omega t \quad (9a) \\ \ddot{y} + \omega_y^2 y + \epsilon \mu \dot{y} - \epsilon (\mu_1 \dot{x}_{\tau_2} + 2\mu_2 \dot{x}_{\tau_2} \dot{y}_{\tau_2} + \mu_3 \dot{y}_{\tau_2} x_{\tau_1} + \alpha_1 x_{\tau_1} + \mu_3 x_{\tau_1} \dot{y}_{\tau_2} + 2\alpha_2 x_{\tau_1} y_{\tau_1}) x - \end{aligned}$$

$$\begin{aligned} & \varepsilon(\mu_2 \dot{x}_{\tau_2}^2 + \alpha_2 x_{\tau_1}^2 + 3\mu_2 \dot{y}_{\tau_2}^2 + 3\alpha_2 y_{\tau_1}^2 + \\ & \sqrt{2}\mu_1 \dot{y}_{\tau_2} + \sqrt{2}\alpha_1 y_{\tau_1} + \mu_1 \dot{y}_{\tau_2} + \alpha_1 y_{\tau_1} + \\ & \mu_3 x_{\tau_1} \dot{x}_{\tau_2} + 3\mu_3 y_{\tau_1} \dot{y}_{\tau_2})y + \varepsilon[\beta_3 x^2 + \\ & 3\mu_4 x^2 \dot{y}_{\tau_2} + \alpha_3 x^2 y_{\tau_1} + (\sqrt{2} + 1)\beta_3 y^2 + \\ & 9\mu_4 \dot{y}_{\tau_2} y^2 + 3\alpha_3 y_{\tau_1} y^2 + 6\mu_4 \dot{x}_{\tau_2} x y + \\ & 2\alpha_3 x_{\tau_1} x y - \beta_2 y^3 - \beta_2 x^2 y + 4\mu_4 \dot{y}_{\tau_2}] = \\ & \varepsilon \Omega^2 \sin \Omega t \end{aligned} \quad (9b)$$

其中  $x_{\tau_1}$ ,  $y_{\tau_1}$  分别代表  $x(t - \tau_1)$ ,  $y(t - \tau_1)$ ,  $\dot{x}_{\tau_2}$ ,  $\dot{y}_{\tau_2}$  分别代表  $\dot{x}(t - \tau_2)$ ,  $\dot{y}(t - \tau_2)$ . 式(9)中各参数表达式见附录公式(2).

## 1.2 多尺度法摄动分析

应用多尺度法<sup>[15]</sup>求解无量纲振动方程(9),选取两个时间尺度,假设解为下列形式:

$$\begin{aligned} x(t, \varepsilon) &= x_0(T_0, T_1) + \varepsilon x_1(T_0, T_1) + O(\varepsilon^2) \\ x(t - \tau_j, \varepsilon) &= x_{0\tau_j}(T_0 - \tau_j, T_1 - \varepsilon\tau_j) + \\ & \varepsilon x_{1\tau_j}(T_0 - \tau_j, T_1 - \varepsilon\tau_j) + O(\varepsilon^2) \quad j=1,2 \\ y(t, \varepsilon) &= y_0(T_0, T_1) + \varepsilon y_1(T_0, T_1) + O(\varepsilon^2) \\ y(t - \tau_j, \varepsilon) &= y_{0\tau_j}(T_0 - \tau_j, T_1 - \varepsilon\tau_j) + \\ & \varepsilon y_{1\tau_j}(T_0 - \tau_j, T_1 - \varepsilon\tau_j) + O(\varepsilon^2) \quad j=1,2 \end{aligned} \quad (10)$$

其中  $T_0 = t$ ,  $T_1 = \varepsilon t$ .  $T_0$  为快时间尺度,  $T_1$  为慢时间尺度.

方程(9)中对时间的微分可通过(11)转化到新的时间尺度上.

$$\frac{d}{dt} = D_0 + \varepsilon D_1, \quad \frac{d^2}{dt^2} = D_0^2 + 2\varepsilon D_0 D_1 + \varepsilon^2 D_1^2 \quad (11)$$

其中  $D_j = \frac{\partial}{\partial T_j}$ ,  $j=0,1$ .

将(10),(11)带入方程(9)中,整理后分离  $\varepsilon$  的同次幂:

$$\varepsilon^0 \text{ 为 } D_0^2 x_0 + \omega_1^2 x_0 = 0 \quad (12a)$$

$$D_0^2 y_0 + \omega_2^2 y_0 = 0 \quad (12b)$$

$\varepsilon^1$  为

$$\begin{aligned} D_0^2 x_1 + \omega_1^2 x_1 &= -2D_0 D_1 x_0 - \mu D_0 x_0 + \\ & 6\mu_3 x_0 x_{0\tau_1} D_0 x_{0\tau_2} + \mu_3 y_0 y_{0\tau_1} D_0 x_{0\tau_2} + \mu_3 (x_0 y_{0\tau_1} + \\ & y_0 x_{0\tau_1}) D_0 y_{0\tau_2} + \alpha_1 (x_0 y_{0\tau_1} + y_0 x_{0\tau_1}) - \\ & \alpha_3 x_{0\tau_1} y_0^2 - 3\alpha_3 x_0^2 x_{0\tau_1} + \alpha_2 x_0 y_{0\tau_1}^2 + \\ & 3\alpha_2 x_0 x_{0\tau_1}^2 + 2\alpha_2 y_0 y_{0\tau_1} x_{0\tau_1} - 2\alpha_3 x_0 y_0 y_{0\tau_1} + \\ & \beta_1 x_0^3 + \beta_2 x_0 y_0^2 - 2\beta_3 x_0 y_0 - 4\mu_4 D_0 x_{0\tau_2} - \end{aligned}$$

$$\begin{aligned} & 9\mu_4 x_0^2 D_0 x_{0\tau_2} - 3\mu_4 y_0^2 D_0 x_{0\tau_2} + 3\mu_2 x_0 D_0 x_{0\tau_2}^2 + \\ & 3\mu_3 x_0 x_{0\tau_1} D_0 x_{0\tau_2} + \mu_1 y_0 D_0 x_{0\tau_2} + \\ & \mu_1 x_0 D_0 y_{0\tau_2} + \mu_2 x_0 D_0 y_{0\tau_2}^2 + \\ & 2\mu_2 y_0 D_0 y_{0\tau_2} D_0 x_{0\tau_2} - 6\mu_4 x_0 y_0 D_0 y_{0\tau_2} + \\ & \varepsilon \Omega^2 \cos(\Omega t) \end{aligned} \quad (13a)$$

$$\begin{aligned} D_0^2 y_1 + \omega_2^2 y_1 &= -2D_0 D_1 y_0 - \mu D_0 y_0 - \\ & \alpha_3 x_0^2 y_{0\tau_1} - 3\alpha_3 y_0^2 y_{0\tau_1} + \alpha_2 y_0 x_{0\tau_1}^2 + \\ & 3\alpha_2 y_0 y_{0\tau_1}^2 + \mu_3 x_0 x_{0\tau_1} D_0 y_{0\tau_2} + \\ & 3\mu_3 y_0 y_{0\tau_1} D_0 y_{0\tau_2} + \mu_3 (x_0 y_{0\tau_1} + \\ & y_0 x_{0\tau_1}) D_0 x_{0\tau_2} + \alpha_1 (x_0 x_{0\tau_1} + y_0 y_{0\tau_1}) - \\ & 2\alpha_3 x_0 y_0 x_{0\tau_1} + 2\alpha_2 x_0 x_{0\tau_1} y_{0\tau_1} + \sqrt{2}\alpha_1 y_0 y_{0\tau_1} + \\ & 2\mu_2 x_0 D_0 y_{0\tau_2} D_0 x_{0\tau_2} + \sqrt{2}\mu_1 y_0 D_0 y_{0\tau_2} - \\ & 6\mu_4 x_0 y_0 D_0 x_{0\tau_2} - 4\mu_4 D_0 y_{0\tau_2} - (\sqrt{2} + \\ & 1)\beta_3 y_0^2 + \beta_2 y_0^3 + \beta_2 x_0^2 y_0 + 3\mu_2 y_0 D_0^2 y_{0\tau_2} + \\ & \mu_2 y_0 D_0^2 x_{0\tau_2} - 3\mu_4 x_0^2 D_0 y_{0\tau_2} - 9\mu_4 y_0^2 D_0 y_{0\tau_2} - \\ & \beta_3 (x_0^2 + y_0^2) + \mu_1 (x_0 D_0 x_{0\tau_2} + y_0 D_0 y_{0\tau_2}) + \\ & \varepsilon \Omega^2 \sin \Omega t \end{aligned} \quad (13b)$$

方程(12)的解为

$$\begin{aligned} x_0 &= A_x(T_1) e^{i\omega_1 T_0} + \bar{A}_x(T_1) e^{-i\omega_1 T_0} \\ y_0 &= A_y(T_1) e^{i\omega_2 T_0} + \bar{A}_y(T_1) e^{-i\omega_2 T_0} \end{aligned} \quad (14)$$

其中  $A_x = a_x/2 \cdot e^{i\beta_x}$ ,  $A_y = a_y/2 \cdot e^{i\beta_y}$ ,  $\bar{A}_x, \bar{A}_y$  分别是  $A_x, A_y$  的共轭,  $i$  为虚数单位. 因此, 相应有:

$$\begin{aligned} x_{0\tau_j} &= A_x(T_1 - \varepsilon\tau_j) e^{i\omega_1(T_0 - \tau_j)} + \bar{A}_x(T_1 - \\ & \varepsilon\tau_j) e^{-i\omega_1(T_0 - \tau_j)}, \quad j=1,2 \\ y_{0\tau_j} &= A_y(T_1 - \varepsilon\tau_j) e^{i\omega_2(T_0 - \tau_j)} + \bar{A}_y(T_1 - \\ & \varepsilon\tau_j) e^{-i\omega_2(T_0 - \tau_j)}, \quad j=1,2 \end{aligned} \quad (15)$$

对  $A_x(T_1 - \varepsilon\tau_j)$  和  $A_y(T_1 - \varepsilon\tau_j)$  进行 Taylor 展开, 由于  $\varepsilon\tau_j \ll 1$ , 为方便推导有

$$\begin{aligned} A_x(T_1 - \varepsilon\tau_j) &= A_x(T_1) - \varepsilon\tau_j D_1 A_x(T_1) + \dots \approx A_x(T_1) \\ A_y(T_1 - \varepsilon\tau_j) &= A_y(T_1) - \varepsilon\tau_j D_1 A_y(T_1) + \dots \approx A_y(T_1) \end{aligned} \quad (16)$$

考虑系统处于主共振、内共振、同时共振情况. 为描述  $\Omega, \omega_2$  与  $\omega_1$  的接近程度, 引入频率调谐参数  $\sigma_1$  和  $\sigma_2$ , 满足下列关系

$$\Omega = \omega_1 + \varepsilon\sigma_1, \quad \omega_2 = \omega_1 + \varepsilon\sigma_2 \quad (17)$$

将式(14)~(17)带入式(13), 得到去除永年项的条件. 分离其实虚部, 并引入  $\beta_x(T_1) = \varepsilon\sigma_1 T_0 - \theta_x(T_1)$ ,  $\beta_y(T_1) = \theta_y(T_1) + \varepsilon(\sigma_1 - \sigma_2) T_0$ , 得到四个自治微分方程, 见附录公式(3).

在上面得到的四个自治微分方程中, 令  $\theta'_x =$

$\theta'_y = a'_x = a'_y = 0$  得到四个代数方程,因为此代数方程组并没有封闭解,因此利用 Newton-Raphson 方法<sup>[16]</sup>求解上述代数方程组,得到系统稳态解  $[\theta_{x0}, a_{x0}, \theta_{y0}, a_{y0}]$ . 上述所得周期解的稳定性可以通过 Lyapunov 第一方法进行判定,假设平衡点  $[\theta_{x0}, a_{x0}, \theta_{y0}, a_{y0}]$ . 将  $\theta_n = \theta_{n0} + \theta_{n1}, a_n = a_{n0} + a_{n1} (n=x, y)$  带入附录中公式(3),其中  $\dot{\theta}_n = \dot{\theta}_{n1}, \dot{a}_n = \dot{a}_{n1}$ . 因此得到在平衡点  $[\theta_{x0}, a_{x0}, \theta_{y0}, a_{y0}]$  处关于摄动项的线性化方程

$$[\dot{\theta}_{x1}, \dot{a}_{x1}, \dot{\theta}_{y1}, \dot{a}_{y1}]^T = [J] [\theta_{x1}, a_{x1}, \theta_{y1}, a_{y1}]^T \quad (18)$$

若式(18)中矩阵  $J$  的所有特征值均具有负实部,则该解为稳定解,否则为不稳定解.

## 2 计算结果及分析

为分析时滞反馈控制对转子-电磁轴承系统的作用,求解上述所得四个自治微分方程[见附录公式(3)]得到近似解,并利用 MATLAB 中 ode45

( $\tau=0$ )求解器及 dde23( $\tau>0$ )求解器<sup>[17]</sup>求解式(9)以验证相同参数下利用多尺度法所得近似解. 计算所用基本参数为:  $k_p = 1.5, k_d = 0.005, i_0 = 0.2, \epsilon = 0.1, \mu = 0.01, \sigma_1 = 0$ . 如无特别说明,在下面的分析图中实线代表稳定解,虚线代表不稳定解. 为了分析方便,本文认为无量纲位移信号时滞量  $\tau_1$  与无量纲速度信号时滞量  $\tau_2$  相等,即  $\tau_1 = \tau_2 = \tau$ .

图 3 展示了水平和垂直方向稳态幅值随时滞量的变化曲线,时滞量的最大取值为转动周期. 可以看到不同的时滞量会导致不同的振动幅值,并且稳定性也不同. 定义使振幅小于  $\tau=0$  时振幅的时滞范围为时滞量的“减振区域”. 图 3 中标注“Suppression range”的范围内,任意一个时滞量下的振动幅值均小于  $\tau=0$  时幅值,说明此时时滞有助于减小系统的振动.  $x$  方向该区域是  $\tau \in [1.74, 2.80]$ ,  $y$  方向该区域是  $\tau \in [1.74, 3.18]$ , 可见在  $x$  和  $y$  方向上虽然稳定解的范围一致,但“减振区域”并不一样,这是由于  $x$  与  $y$  方向上受力不同.

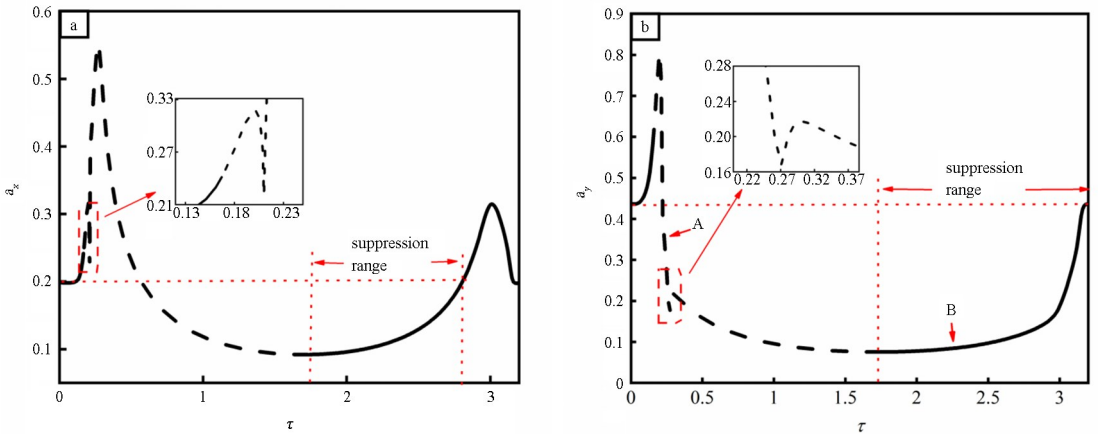


图 3 无量纲时滞量-无量纲幅值曲线(实线代表稳定解,虚线代表不稳定解)

Fig.3 Dimensionless time delay-dimensionless amplitude curves

(The solid line represents the stable solution, the dash line represents the unstable solution)

图 4 展示了控制器中比例增益  $k_p$  为 1.3, 1.5, 1.8 和 2.2 时的曲线,图 5 展示了微分增益为 0.003, 0.005, 0.008 和 0.012 时的曲线. 对比之下,比例系数变化时曲线的形状变化更大. 表 1 和表 2 分别统计了图 4、图 5 中减振区域的区间,可以看到比例系数变化时减振区域的变化更大,当  $k_p$  为 2.2 时减振区域由不连续的四个区间组成. 对比表 1 和表 2,微分系数增大对于减振区域影响较小,适当增大微分增益有助于提高系统阻尼,也可减小系统的振

动幅值,但减振效果有限,因为过大的微分增益同时也放大了系统的高频噪声,使系统性能恶化.

表 1 不同  $k_p$  的减振区域

$k_p$	减振区域
1.3	[2.34 3.97]
1.5	[1.74 2.80]
1.8	[1.34 2.24]
2.2	(0 0.31] [1.04 1.83] [2.04 2.35] [3.13 3.84]



表2 不同  $k_d$  的减振区域

Table 2 Suppression region at different values of  $k_d$

$k_d$	减振区域
0.003	[1.67 2.82]
0.005	[1.74 2.80]
0.008	[1.84 2.89]
0.012	[1.98 2.93]

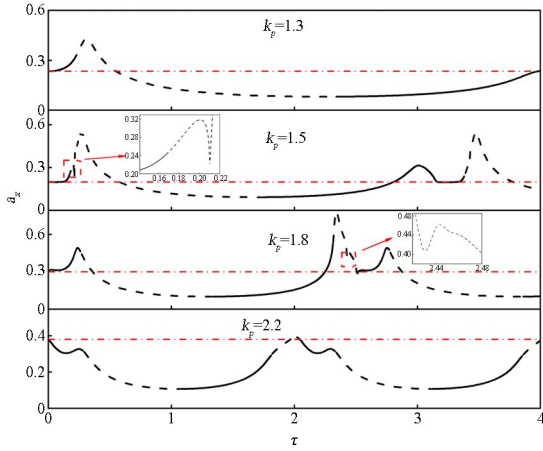


图4 不同比例增益  $k_p$  时  $\tau$ - $a_x$  曲线

Fig.4  $\tau$ - $a_x$  curves at different proportional gains  $k_p$

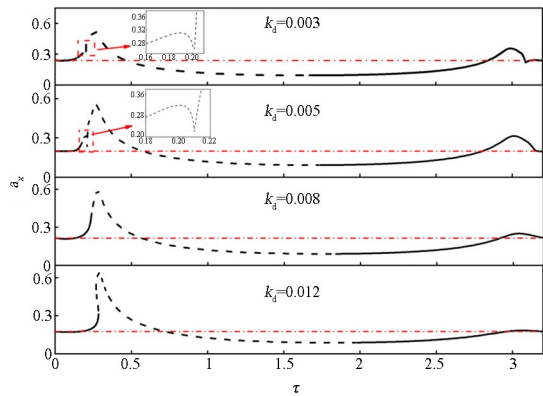


图5 不同微分增益  $k_d$  时  $\tau$ - $a_x$  曲线

Fig.5  $\tau$ - $a_x$  curves at different differential gains  $k_d$

上面研究了转速与系统固有频率相等( $\sigma_1=0$ )情况下的减振效果,为研究其他转速下是否也具有减振效果,图6展示了图3(b)中A,B两点代表的时滞量以及情况下的幅频特性曲线.当 $\tau=0$ 时,系统在各转速范围内均稳定且幅值较小,而当时滞量为0.23时(点A),系统的共振区幅值明显增大,且在 $\sigma_1 \in [-0.052, 0.052]$ 范围内失去稳定性,这对转子的安全稳定运行造成很大威胁.当时滞量为2.3时(点B),系统在水平和垂直方向上主共振峰值均大幅减小,但当转速远离主共振情况时,时滞控制的效果不一定好,如图6(a)中 $\sigma_1 = -0.1, \tau = 2.3$

的幅值要高于无时滞振幅.

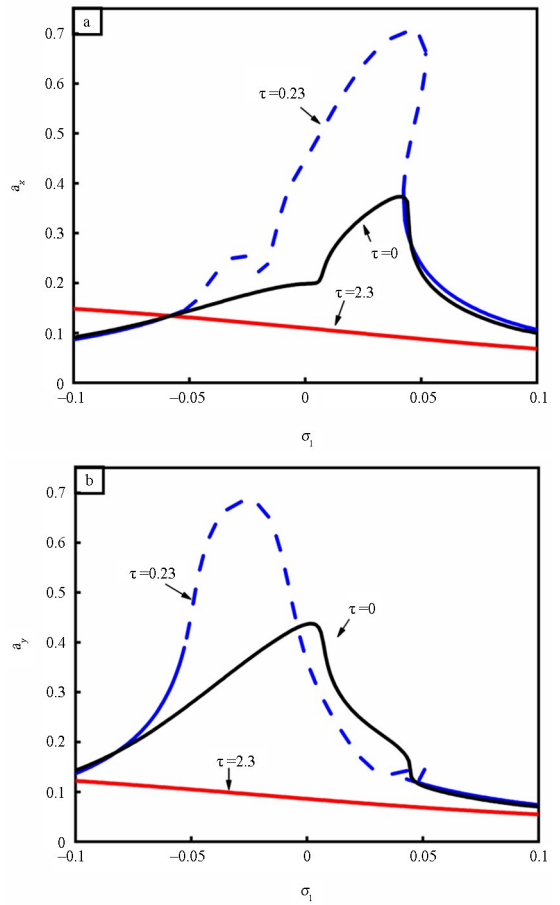


图6 不同转速下时滞控制的效果

Fig.6 Effect of time delay control at different rotation speeds

图7展示了不同转速下时滞的“减振区域”.  $x$ 和 $y$ 方向上“减振区域”的分布并不相同,上方区域面积较大,包括了大多数 $\sigma_1$ 取值. $x$ 方向的上方减振区域左侧边界为 $\sigma_1 = -0.06$ ,而在 $\sigma \in [-0.1, -0.06]$ 区间内只有下方减振区域.图6和图7说明在转速变化时同一时滞量做不到全范围减振,此时可能根据需要进行时滞量参数的变化以适应减振需求.但在 $y$ 方向上合适的时滞量是能做到 $\sigma \in [-0.1, 0.1]$ 范围内均减小振动.

转子不平衡是工程中较为常见的一个问题,质量偏心相当于对转子施加一个同频激励,使转子产生强迫振动.工程中若发现转子质量不平衡问题,一般需要停止设备运行并进行动平衡处理,费时费力.磁悬浮轴承具有可施加主动控制的优势,无需硬件改造,只需在算法上进行处理,即可对转子的不平衡响应进行抑制.图7展示了不同转速下时滞对无量纲偏心量-无量纲幅值曲线的影响.时滞量选取了图3“减振区域”中的 $\tau = 2.3$ .当 $\tau=0$ 时,由

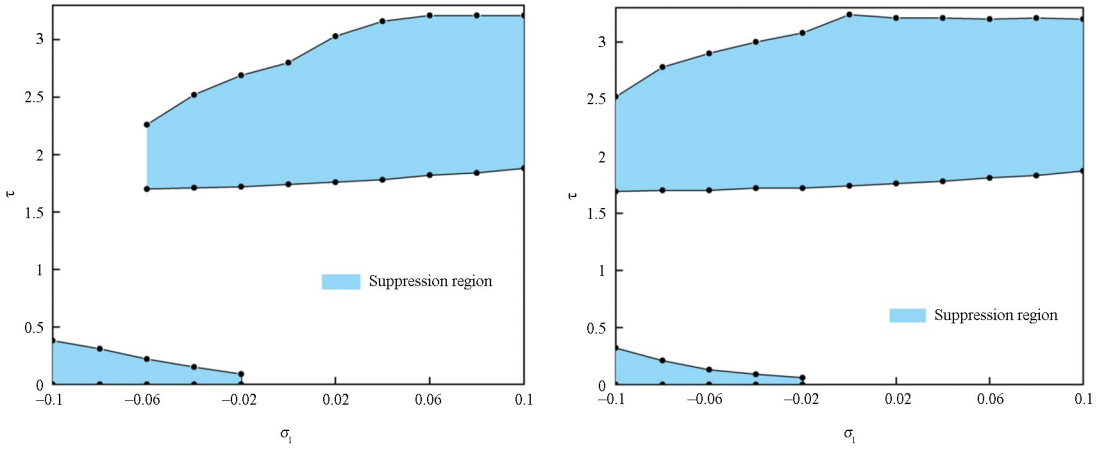


图 7 不同  $\sigma_1$  时的减振区域图  
Fig.7 Suppression region at different  $\sigma_1$

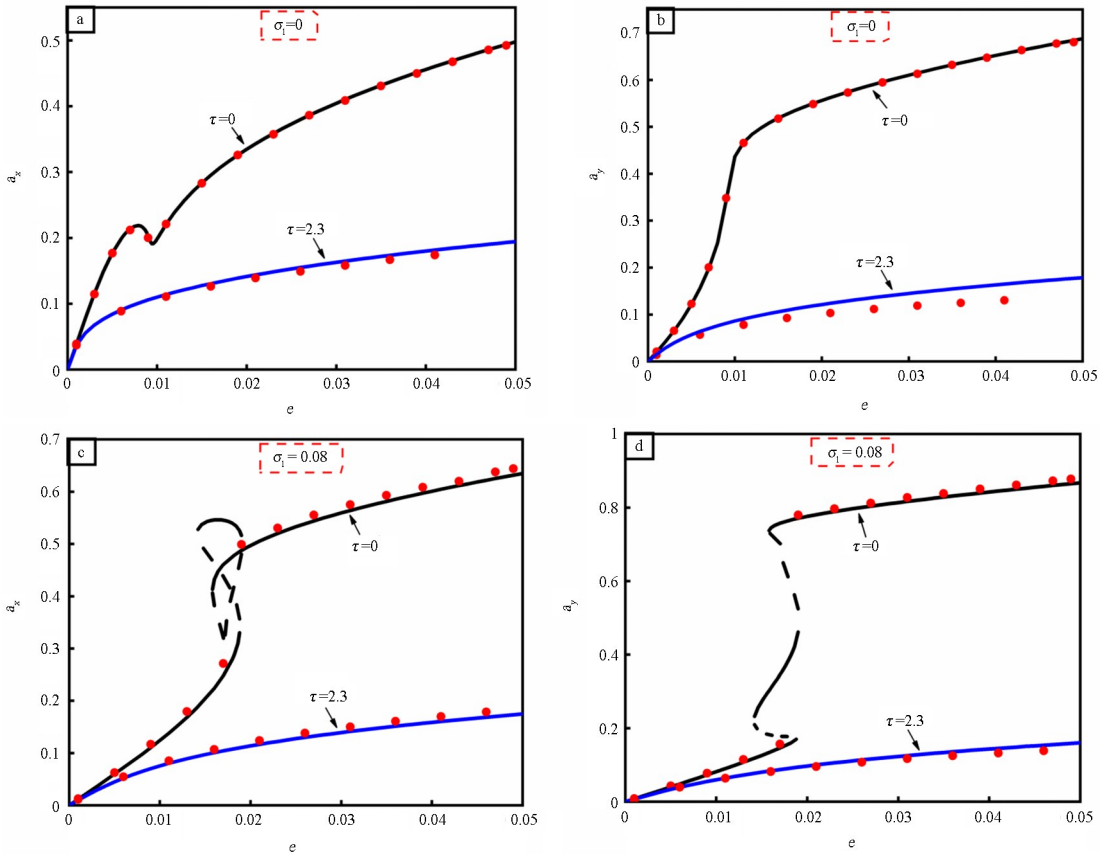


图 8 加入时滞控制前后转子偏心量  $e$ —幅值曲线(红点表示数值模拟解)  
Fig.8 Eccentricity-amplitude curve before and after considering time delay  
(Red dots indicate numerical simulation solutions)

于电磁力的非线性以及电磁轴承的几何耦合,系统表现出许多非线性现象,如多值、突跳现象等.系统在某些转速范围内存在不稳定解,这使系统存在失稳的风险,如图 7(c)(d)中虚线所示.当  $\sigma_1$  时随着偏心量的增加转子振动幅值总体趋势是增大的,这是因为偏心量的增加相当于对转子的激励增大,因此振动幅值增大.当采用传统 PD 控制时( $\tau=0$ ),系

统在各偏心率下均保持稳定,但幅值较大;采用时滞反馈控制后( $\tau=2.3$ ),系统在水平和竖直方向幅值均降低.当  $\sigma_1=0.08$  时系统响应的对比,如图 7(c)(d).采用线性 PD 控制时( $\tau=0$ ),系统特性曲线出现不稳定区域,说明系统在某些偏心量下可能会发生失稳.加入时滞控制后( $\tau=2.3$ ),不稳定区域消失,同时各偏心率对应的振动幅值也大大减小.

红点表示通过 MATLAB 中 dde23 求得的数值积分解,与多尺度法所得近似解吻合良好.以上分析说明了时滞反馈控制对于最常见的转子不平衡问题具有良好的抑制作用.

### 3 结论

本文建立了时滞反馈控制下高速转子—电磁轴承系统的非线性模型,利用多尺度法求得方程的近似解并进行稳定性判定,利用 MATLAB 中 dde23 求解器验证近似解的准确性.主要研究了时滞反馈控制对于系统主共振峰值及稳定性的影响,并对时滞量的选取进行了分析,同时考察了时滞反馈控制对工程中最常见的转子不平衡问题的控制效果.主要结论如下:

(1)相对于微分增益,比例增益  $k_p$  对时滞量“减振区域”影响较大.

(2)在某些时滞量取值下,转子振动幅值增大直至失稳,当时滞量取在“减振区域”时有助于减小转子振动幅值,增强运行稳定性.由于受力的不同,水平和竖直方向上“减振区域”并不相同.

(3)时滞反馈控制对于转子—电磁轴承系统的主共振峰值具有良好的抑制作用,但当转速变化时同一时滞量可能失去减振作用.

(4)时滞反馈控制对转子不平衡响应具有显著的控制效果,并且消除了一些非线性现象如多值、突跳等,具有广阔的应用前景.

在高速转子—电磁轴承系统的振动控制中,相对于其他复杂的控制算法,时滞反馈控制相对简单且容易理解.本文的研究结果表明其减振效果好,具有广阔的应用前景,但伴随而来的问题是若时滞量取的不好甚至不对,系统将会失去稳定性.系统非线性与时滞的联合作用使得系统非常复杂,目前对于时滞量取值的理论指导还较少,多数情况下要依靠数值模拟结果,为此需要更多的研究.

### 参考文献

[1] KANG G S, CUI X Z. Computing time delay and its effect on real-time control systems [J]. IEEE Transactions on Control Systems Technology, 1995, 3(2):218—224.

[2] 胡海岩,王在华.非线性时滞动力系统的研究进展

[J].力学进展, 1999,29(4):501—512.

HU H Y, WANG Z H. Review on nonlinear dynamic systems involving time delays [J]. Advances in Mechanics, 1999, 29(4):501—512. (in Chinese)

[3] JI J C. Dynamics of a Jeffcott rotor-magnetic bearing system with time delays [J]. International Journal of Non-linear Mechanics, 2013, 38(9):1387—1401.

[4] SAEED N A, EI-GANINI W A, EISSA M. Nonlinear time delay saturation-based controller for suppression of nonlinear beam vibrations [J]. Applied Mathematical Modelling, 2013, 37(20—21):8846—8864.

[5] SAEED N A, EI-GANINI W A. Time-delayed control to suppress the nonlinear vibrations of a horizontally suspended Jeffcott-rotor system [J]. Applied Mathematical Modelling, 2017, 44:523—539.

[6] SAEED N A, MOATIMID G M, ELSABAA F M F, et al. Time-delayed control to suppress a nonlinear system vibration utilizing the multiple scales homotopy approach [J]. Archive of Applied Mechanics, 2021, 91(3):1193—1215.

[7] 刘显波.大柔性细长转子系统时滞非线性动力学及主动控制 [D].上海:上海交通大学,2017.

LIUX B. Dynamics and control of a slender, flexible rotor with time-delay effects [D]. Shanghai: Shanghai Jiao Tong University, 2017. (in Chinese)

[8] AMER Y A, EI-SAYED A T, KOTB A A. Nonlinear vibration and of the Duffing oscillator to parametric excitation with time delay feedback [J]. Nonlinear Dynamics, 2016, 85(4):2497—2505.

[9] AMER Y A, EI-SAYED A, ABD EI-SALAM M N. Position and velocity time delay for suppression vibrations of a hybrid Rayleigh-Van der Pol-Duffing oscillator [J]. Sound and Vibration, 2020, 54(3):149—161.

[10] 赵艳影,徐鉴.时滞非线性动力吸振器的减振机理 [J].力学学报, 2008, 40(1):98—106.

ZHAO Y Y, XU J. Mechanism analysis of delayed nonlinear vibration absorber [J]. Chinese Journal of Theoretical and Applied Mechanics, 2008, 40(1):98—106. (in Chinese)

[11] YAN G, FANG M X. Analysis and experiment of time-delayed optimal control for vehicle suspension system [J]. Journal of Sound and Vibration, 2019, 446:144—158.

[12] 邵素娟,任传波,荆栋.时滞非线性主动悬架系统的减振控制研究 [J].应用力学学报, 2021, 38(3):



1218—1225.

SHAO S J, REN C B, JING D. Vibration control of nonlinear active suspension system with time delay [J]. Chinese Journal of Applied Mechanics, 2021, 38 (3): 1218—1225. (in Chinese)

[13] ZHANG W, ZHAN X P. Periodic and chaotic motions of a rotor-active magnetic bearing with quadratic and cubic terms and time-varying stiffness [J]. Nonlinear Dynamics, 2005, 41: 331—359.

[14] ZHENG K, YU L. Effects of time delay on resonance of a nonlinear magnetic bearing system with delayed feedback [J]. International Journal of Applied Electromagnetics and Mechanics, 2010, 33:

1547—1554.

[15] 胡海岩. 应用非线性动力学 [M]. 北京: 航空工业出版社, 2000.

HU H Y. Applied nonlinear dynamics [M]. Beijing: Aviation Industry Press, 2000. (in Chinese)

[16] 韩丹夫. 数值计算方法 [M]. 浙江: 浙江大学出版社, 2006.

HAN D. Numerical computing methods [M]. Zhejiang: Zhejiang University Press, 2006. (in Chinese)

[17] SHAMPINE L F, THOMPSON S. Solving DDEs in MATLAB [J]. Applied Numerical Mathematics, 2001, 37(4): 441—458.

## 附录:

### 1 无量纲振动方程:

$$\ddot{x} = \frac{[1 - k_p x(t - \tau_1) - k_d \dot{x}(t - \tau_2)]^2}{(1 - x(t))^2} - \frac{[1 + k_p x(t - \tau_1) + k_d \dot{x}(t - \tau_2)]^2}{(1 + x(t))^2} + \frac{\sqrt{2}}{2} \left[ \frac{\left\{ 1 - i_0 - \frac{\sqrt{2}}{2} (k_p [x(t - \tau_1) + y(t - \tau_1)] + k_d [\dot{x}(t - \tau_2) + \dot{y}(t - \tau_2)]) \right\}^2}{\left\{ 1 - \frac{\sqrt{2}}{2} [x(t) + y(t)] \right\}^2} - \frac{\left( 1 + i_0 + \frac{\sqrt{2}}{2} \{ k_p [x(t - \tau_1) + y(t - \tau_1)] + k_d [\dot{x}(t - \tau_2) + \dot{y}(t - \tau_2)] \} \right)^2}{\left\{ 1 + \frac{\sqrt{2}}{2} [x(t) + y(t)] \right\}^2} - \frac{\left\{ 1 - i_0 - \frac{\sqrt{2}}{2} \{ k_p [y(t - \tau_1) - x(t - \tau_1)] + k_d [\dot{y}(t - \tau_2) - \dot{x}(t - \tau_2)] \} \right\}^2}{\left\{ 1 - \frac{\sqrt{2}}{2} [y(t) - x(t)] \right\}^2} + \frac{\left\{ 1 + i_0 + \frac{\sqrt{2}}{2} \{ k_p [y(t - \tau_1) - x(t - \tau_1)] + k_d [\dot{y}(t - \tau_2) - \dot{x}(t - \tau_2)] \} \right\}^2}{\left\{ 1 + \frac{\sqrt{2}}{2} [y(t) - x(t)] \right\}^2} \right] - c\dot{x} + e\Omega^2 \cos(\Omega t) \quad (1a)$$

$$\ddot{y} = \frac{[1 - i_0 - k_p y(t - \tau_1) - k_d \dot{y}(t - \tau_2)]^2}{[1 - y(t)]^2} - \frac{[1 + i_0 + k_p y(t - \tau_1) + k_d \dot{y}(t - \tau_2)]^2}{[1 + y(t)]^2} + \frac{\sqrt{2}}{2} \left[ \frac{\left\{ 1 - i_0 - \frac{\sqrt{2}}{2} \{ k_p [x(t - \tau_1) + y(t - \tau_1)] + k_d [\dot{x}(t - \tau_2) + \dot{y}(t - \tau_2)] \} \right\}^2}{\left\{ 1 - \frac{\sqrt{2}}{2} [x(t) + y(t)] \right\}^2} - \frac{\left( 1 + i_0 + \frac{\sqrt{2}}{2} \{ k_p [x(t - \tau_1) + y(t - \tau_1)] + k_d [\dot{x}(t - \tau_2) + \dot{y}(t - \tau_2)] \} \right)^2}{\left\{ 1 + \frac{\sqrt{2}}{2} [x(t) + y(t)] \right\}^2} + \frac{\left\{ 1 - i_0 - \frac{\sqrt{2}}{2} \{ k_p [x(t - \tau_1) + y(t - \tau_1)] + k_d [\dot{x}(t - \tau_2) + \dot{y}(t - \tau_2)] \} \right\}^2}{\left\{ 1 - \frac{\sqrt{2}}{2} [x(t) + y(t)] \right\}^2} + \frac{\left( 1 + i_0 + \frac{\sqrt{2}}{2} \{ k_p [x(t - \tau_1) + y(t - \tau_1)] + k_d [\dot{x}(t - \tau_2) + \dot{y}(t - \tau_2)] \} \right)^2}{\left\{ 1 + \frac{\sqrt{2}}{2} [x(t) + y(t)] \right\}^2} \right]$$

$$\begin{aligned}
& \left\{ 1 - \frac{i_0}{I_0} - \frac{\sqrt{2}}{2} \{ k_p [y(t - \tau_1) - x(t - \tau_1)] + k_d [\dot{y}(t - \tau_2) - \dot{x}(t - \tau_2)] \} \right\}^2 \\
& \quad \left\{ 1 - \frac{\sqrt{2}}{2} [y(t) - x(t)] \right\}^2 \\
& \left. \left[ \frac{\left\{ 1 + i_0 + \frac{\sqrt{2}}{2} \{ k_p [y(t - \tau_1) - x(t - \tau_1)] + k_d [\dot{y}(t - \tau_2) - \dot{x}(t - \tau_2)] \} \right\}^2}{\left\{ 1 + \frac{\sqrt{2}}{2} [y(t) - x(t)] \right\}^2} \right] - \right. \\
& c\dot{y} + 4(\sqrt{2} + 1)i_0 + e\Omega^2 \sin(\Omega t)
\end{aligned} \tag{1b}$$

2 式(9)中各参数意义:

$$\begin{aligned}
\mu_1 &= 4\sqrt{2}i_0k_d, \alpha_1 = 4\sqrt{2}i_0k_p, \mu_2 = 2k_d^2, \mu_3 = 4k_pk_d, \alpha_2 = 2k_p^2, \mu_4 = 2k_d, \alpha_3 = 6k_p, \beta_1 = 12 + 4i_0^2, \\
\beta_2 &= 12 + 12i_0^2, \beta_3 = 6\sqrt{2}i_0, \mu = c - 8k_p\tau_1, \omega_1^2 = 8k_p - 8 - 4i_0^2, \omega_2^2 = 8k_p - 8 - 8i_0^2
\end{aligned} \tag{2}$$

3 利用多尺度法得到的自治微分方程:

$$\begin{aligned}
a_x \omega_1 \theta'_x &= a_x [\omega_1 \sigma_1 - 16\Gamma_6 \sin(\Psi_3)] + a_x a_y^2 [2\Gamma_5 \cos(\Psi_{15} - 2\theta_x - 2\theta_y) + 2\Gamma_5 \cos(\Psi_{15}) - \Gamma_4 \cos(2\Psi_4 - \\
& 2\theta_x - 2\theta_y) - 2\Gamma_5 \cos(\Psi_6) - 2\Gamma_{12} \sin(\Psi_{16}) + \Gamma_{12} \sin(\Psi_{13}) + \Gamma_{12} \sin(\Psi_{11}) + \Gamma_{12} \sin(\Psi_{12} - 2\theta_x - 2\theta_y) + \\
& \Gamma_{12} \sin(\Psi_{13} - 2\theta_x - 2\theta_y) - 6\Gamma_7 \sin(\Psi_4 - 2\theta_y - 2\theta_x) - 12\Gamma_7 \sin(\Psi_4) - 3\Gamma_6 \sin(\Psi_3 + 2\theta_x + 2\theta_y) - \\
& \Gamma_1 \cos(\Psi_1 + 2\theta_x + 2\theta_y) - 4\Gamma_1 \cos(\Psi_2) - 2\Gamma_1 \cos(\Psi_2 - 2\theta_x - 2\theta_y) - 3\Gamma_{11} \sin(\Psi_7 - 2\theta_x - 2\theta_y) - \\
& \Gamma_{11} \sin(\Psi_7) + \Gamma_{11} \sin(\Psi_{10}) + 2\Gamma_2 + 2\Gamma_{10} + 2\Gamma_2 \cos(\Psi_5) + \Gamma_2 \cos(2\Psi_2 - 2\theta_x - 2\theta_y) + 2\Gamma_2 \cos(\Psi_{14} - \\
& 2\theta_x - 2\theta_y) + 2\Gamma_2 \cos(\Psi_{14}) + \Gamma_{10} \cos(2\theta_x + 2\theta_y) + 2\Gamma_4 - 6\Gamma_6 \sin(\Psi_3) - 2\Gamma_1 a_x a_y^2 \cos(\Psi_1)] + \\
& a_x^3 [-3\Gamma_3 \cos(2\Psi_3) - 9\Gamma_1 \cos(\Psi_1) + 6\Gamma_{11} \sin(\Psi_{13}) + 3\Gamma_{11} \sin(\Psi_9) + 6\Gamma_2 + \Gamma_9 + 3\Gamma_2 \cos(2\Psi_1) + \\
& 6\Gamma_3 - 27\Gamma_6 \sin(\Psi_3)] + \frac{1}{2} e\Omega^2 \cos(\theta_x)
\end{aligned} \tag{3a}$$

$$\begin{aligned}
\omega_1 a'_x &= a_x \left[ -\frac{\mu}{2} \omega_1 - 16\Gamma_6 \cos(\Psi_3) \right] + a_x a_y^2 [3\Gamma_6 \cos(\Psi_3 + 2\theta_x + 2\theta_y) + \Gamma_{11} \cos(\Psi_7) + \Gamma_{11} \cos(\Psi_{10}) - \\
& \Gamma_{11} \cos(\Psi_7 - 2\theta_x - 2\theta_y) - \Gamma_1 \sin(\Psi_1 + 2\theta_x + 2\theta_y) + 2\Gamma_1 \sin(\Psi_2 - 2\theta_x - 2\theta_y) - 2\Gamma_2 \sin(\Psi_5) - \\
& 2\Gamma_5 \sin(\Psi_{15} - 2\theta_x - 2\theta_y) - 2\Gamma_5 \sin(\Psi_{15} - 2\theta_x - 2\theta_y) + \Gamma_4 \sin(2\Psi_4 - 2\theta_x - 2\theta_y) + 2\Gamma_5 \sin(\Psi_{15}) + \\
& 2\Gamma_5 \sin(\Psi_6) - \Gamma_{12} \cos(\Psi_{13}) + \Gamma_{12} \cos(\Psi_{11}) + \Gamma_{12} \cos(\Psi_{12} - 2\theta_x - 2\theta_y) + \Gamma_{12} \cos(\Psi_{13} - 2\theta_x - 2\theta_y) - \\
& 6\Gamma_7 \cos(\Psi_4 - 2\theta_x - 2\theta_y) + 2\Gamma_2 \sin(\Psi_{14}) - \Gamma_2 \sin(2\Psi_2 - 2\theta_x - 2\theta_y) - 2\Gamma_2 \sin(\Psi_{14} - 2\theta_x - 2\theta_y) + \\
& \Gamma_{10} \sin(2\theta_x + 2\theta_y) - 6\Gamma_6 \cos(\Psi_3) + 2\Gamma_1 \sin(\Psi_1)] + a_x^3 [3\Gamma_{11} \cos(\Psi_9) + 3\Gamma_3 \sin(2\Psi_3) + \\
& 3\Gamma_1 \sin(\Psi_1) - 3\Gamma_2 \sin(2\Psi_1) - 9\Gamma_6 \cos(\Psi_3)] + \frac{1}{2} e\Omega^2 \sin(\theta_x)
\end{aligned} \tag{3b}$$

$$\begin{aligned}
-a_y \omega_2 \theta'_y &= a_y [\omega_1 (\sigma_1 - \sigma_2) - 16\Gamma_7 \sin(\Psi_4)] + a_y^2 a_x [-12\Gamma_6 \sin(\Psi_3) - 6\Gamma_6 \sin(\Psi_3 + 2\theta_x + 2\theta_y) - \\
& \Gamma_3 \cos(2\Psi_3 + 2\theta_x + 2\theta_y) + 2\Gamma_5 \cos(\Psi_{15}) + 2\Gamma_5 \cos(\Psi_{15} - 2\theta_x - 2\theta_y) - 2\Gamma_5 \cos(\Psi_6) - 2\Gamma_{11} \sin(\Psi_8) + \\
& \Gamma_{11} \sin(\Psi_{10}) - \Gamma_{11} \sin(\Psi_7) + \Gamma_{11} \sin(\Psi_9 + 2\theta_x + 2\theta_y) - \Gamma_{11} \sin(\Psi_7 - 2\theta_x - 2\theta_y) + \Gamma_{12} \sin(\Psi_{11}) + \\
& \Gamma_{12} \sin(\Psi_{13} - 2\theta_x - 2\theta_y) + \Gamma_{12} \sin(\Psi_{13}) - 4\Gamma_1 \cos(\Psi_1) - \Gamma_1 \cos(\Psi_2 - 2\theta_x - 2\theta_y) - 2\Gamma_1 \cos(\Psi_1 + \\
& 2\theta_x + 2\theta_y) + 2\Gamma_2 \cos(\Psi_5) + 2\Gamma_2 \cos(\Psi_{14} - 2\theta_x - 2\theta_y) + 2\Gamma_2 \cos(\Psi_{14}) + \Gamma_2 \cos(2\Psi_1 + 2\theta_x + 2\theta_y) - \\
& 3\Gamma_7 \sin(\Psi_4 - 2\theta_x - 2\theta_y) + \Gamma_{10} \cos(2\theta_x + 2\theta_y) + 2\Gamma_2 + 2\Gamma_{10} + 2\Gamma_3 - 2\Gamma_1 \cos(\Psi_2) - 6\Gamma_7 \sin(\Psi_4)] + \\
& a_y^3 [6\Gamma_2 + 3\Gamma_{10} + 6\Gamma_4 - 3\Gamma_4 \cos(2\Psi_4) - 6\Gamma_{12} \sin(\Psi_{16}) + 3\Gamma_{12} \sin(\Psi_{12}) - 9\Gamma_1 \cos(\Psi_2) + \\
& 3\Gamma_2 \cos(2\Psi_2) - 27\Gamma_7 \sin(\Psi_4)] - \frac{1}{2} e\Omega^2 \sin(\theta_y)
\end{aligned} \tag{3c}$$

$$\begin{aligned}
\omega_2 a'_y &= a_y \left[ -\frac{\mu}{2} \omega_2 - 16\Gamma_7 \cos(\Psi_4) \right] + a_y^2 a_x [\Gamma_{11} \cos(\Psi_{10}) - \Gamma_{11} \cos(\Psi_7) + \Gamma_{12} \cos(\Psi_{13}) + \Gamma_{12} \cos(\Psi_{11}) + \\
& \Gamma_{11} \cos(\Psi_9 + 2\theta_x + 2\theta_y) + \Gamma_{11} \cos(\Psi_7 - 2\theta_x - 2\theta_y) - \Gamma_{12} \cos(\Psi_{13} - 2\theta_x - 2\theta_y) + 2\Gamma_5 \sin(\Psi_{10}) -
\end{aligned}$$

$$\begin{aligned}
& 2\Gamma_5 \sin(\Psi_{15}) + 2\Gamma_5 \sin(\Psi_{15} - 2\theta_x - 2\theta_y) + \Gamma_3 \sin(2\Psi_3 + 2\theta_x + 2\theta_y) - 2\Gamma_2 \sin(\Psi_{14}) - 2\Gamma_2 \sin(\Psi_5) + \\
& 2\Gamma_2 \sin(\Psi_{14} - 2\theta_x - 2\theta_y) + 2\Gamma_1 \sin(\Psi_1 + 2\theta_x + 2\theta_y) - \Gamma_1 \sin(\Psi_2 - 2\theta_x - 2\theta_y) - 6\Gamma_6 \cos(\Psi_3 + \\
& 2\theta_x + 2\theta_y) + 3\Gamma_7 \cos(\Psi_4 - 2\theta_x - 2\theta_y) - \Gamma_{10} \sin(2\theta_x + 2\theta_y) - \Gamma_2 \sin(2\Psi_1 + 2\theta_x + 2\theta_y) + 2\Gamma_1 \sin(\Psi_2) - \\
& 6\Gamma_7 \cos(\Psi_4)] + a_y^3 [3\Gamma_{12} \cos(\Psi_{12}) + 3\Gamma_4 \sin(2\Psi_4) - 3\Gamma_2 \sin(2\Psi_2) + 3\Gamma_1 \sin(\Psi_2) - 9\Gamma_7 \cos(\Psi_4)] - \\
& \frac{1}{2} e\Omega^2 \cos(\theta_y)
\end{aligned} \tag{3d}$$

上式中各参数说明:

$$\begin{aligned}
\Gamma_1 &= \frac{\alpha_3}{8}, \Gamma_2 = \frac{\alpha_2}{8}, \Gamma_3 = \frac{\mu_2}{8} \omega_1^2, \Gamma_4 = \frac{\mu_2}{8} \omega_2^2, \Gamma_5 = \frac{\mu_2}{8} \omega_1 \omega_2, \Gamma_6 = \frac{\mu_4}{8} \omega_1, \Gamma_7 = \frac{\mu_4}{8} \omega_2, \Gamma_8 = \frac{f_1}{8}, \Gamma_9 = \frac{3\beta_1}{8}, \\
\Gamma_{10} &= \frac{\beta_2}{8}, \Gamma_{11} = \frac{\mu_3}{8} \omega_1, \Gamma_{12} = \frac{\mu_3}{8} \omega_2, \Psi_1 = \omega_1 \tau_1, \Psi_2 = \omega_2 \tau_1, \Psi_3 = \omega_1 \tau_2, \Psi_4 = \omega_2 \tau_2, \Psi_5 = \omega_1 \tau_1 + \omega_2 \tau_1, \\
\Psi_6 &= \omega_1 \tau_2 + \omega_2 \tau_2, \Psi_7 = \omega_2 \tau_1 - \omega_1 \tau_2, \Psi_8 = \omega_1 \tau_1 - \omega_1 \tau_2, \Psi_9 = \omega_1 \tau_1 + \omega_1 \tau_2, \Psi_{10} = \omega_1 \tau_2 + \omega_2 \tau_1, \\
\Psi_{11} &= \omega_1 \tau_1 + \omega_2 \tau_2, \Psi_{12} = \omega_2 \tau_1 + \omega_2 \tau_2, \Psi_{13} = \omega_2 \tau_2 - \omega_1 \tau_1, \Psi_{14} = \varepsilon \sigma_2 \tau_1, \Psi_{15} = \varepsilon \sigma_2 \tau_2, \Psi_{16} = \omega_2 \tau_1 - \omega_2 \tau_2
\end{aligned}$$